The relationship between surface topography and peat thickness on Tebing Tinggi Island, Indonesia

B. Nasrul[1,2], A. Maas[2], S.N.H. Utami[2], M. Nurudin[2]

[1]Study Program of Soil Science, Faculty of Agriculture, Universitas Riau, Tampan, Pekanbaru, Indonesia
[2]Department of Soil Science, Faculty of Agriculture, Universitas Gadjah Mada, Bulaksumur, Yogyakarta, Indonesia

_____

SUMMARY

Peat and its substratum have different geology and parent materials. Studies on peat formation and spatial patterns of peat deposits have been widely reported, but little is known about patterns of peat thickness across tropical peat landscapes. We studied the relationship between surface relief and peat thickness on Tebing Tinggi Island (Indonesia) by considering peat surface altitude, peat thickness and substratum altitude. The research location is unique, being a small (~ 70 × 30 km) predominantly peat-covered island separated by a strait from the mainland of Sumatra and its more extensive peat deposits. Geomorphological features on the island were identified using a digital terrain model (DTM) developed from LiDAR data, together with observations on peat cores. The results indicate that the topography of the peat landscape does not reflect peat thickness. Thick peat can be found at the edge of a peat dome if it overlies a basin or valley in the substratum, while thinner peat can be found at the centre if it overlies a mound in the substratum. It is also important to note that the shapes of the peat surface and the substratum surface are not the same; a flat peatland surface may have an undulating substratum and vice versa.

KEY WORDS: LiDAR DTM, macrotope, peat dome, peat surface altitude, substratum, Sumatra

_____

INTRODUCTION

Tropical peat swamp ecosystems globally cover a total area of 439,238 km^2 and 57 % of this area is distributed across south-east Asia (Rieley *et al.* 2011). These ecosystems store large organic matter reserves (Jaenicke *et al.* 2008) and have unique endemic fauna (Harrison & Rieley 2018), although a possibly less distinctive flora (Giesen *et al.* 2018). Tropical peat is formed in situ by the accumulation of organic matter. It is composed of dead vegetation whose decomposition is curtailed due to waterlogging. The exact degree of natural decomposition is determined by the nature of that waterlogging, i.e. the duration of high and stable local water levels, which is influenced by factors such as proximity to river channels and drainage canals, and in the longer term has been associated with changes in sea level (Maas 2003).

Peat swamps can be morphologically divided into natural levées, back swamps and peat domes. Natural levées are formed by the sedimentation of mineral-rich material alongside river channels, creating distal back swamps with sluggish drainage which have often filled with peat and eventually developed into peat domes with only a fringe of remnant back swamp (Figure 1). Peat domes store rainwater and release it gradually to the surrounding land, and thence to rivers and seas. Thus, they perform an important hydrological regulation function without which surface water and groundwater will become uncontrolled and water reserves will fluctuate sharply during both rainy and dry seasons (Maas 2003).

Peat decomposition is driven by unbalanced hydro-topographical conditions, in which the water supply is less than the sum of evapotranspiration and outflow from the peatland. When peatlands are drained the water table retreats from the peat surface, creating an aerobic environment in which decomposition resumes, releasing carbon to the atmosphere (Hirano *et al.* 2012, Couwenberg & Hooijer 2013) and leading to compaction of the peat (Hooijer *et al.* 2012). The resulting subsidence of the peat surface (e.g. Nagano *et al.* 2013) changes the form of the landscape and affects the dome's hydrology. Geomorphological analysis is useful in studying changes in landscape form brought about by both human and 'natural' drivers, and can be improved using historical techniques (Trimble 2008). Peatlands possess a diversity of topographical forms (Minayeva *et al.* 2017), and the level of the water table in the peat tends to follow surface topography (Strack *et al.* 2008). Thus, the combination of surface topography and substratum material plays a crucial role in hydrological processes by regulating the water storage capacity and the direction of water flow

(Graniero & Price 1999); and understanding the relationship between peat surface topography and peat thickness is very necessary in developing a robust foundation for the management of peatland hydrological units. However, research on the topography, as well as the thickness, of tropical peat and its relationship with the substratum is still limited. Research conducted by Laamrani *et al.* (2014) correlated peat thickness and landscape topography with the level of productivity in black spruce forest growing on largely organic soils in the Northern Canadian boreal forest, and found that productivity was lowest where the organic horizons were deepest. Bragg (1997) identified potential parallels in ecohydrological functioning between temperate raised bog and south-east Asian peat swamp forest domes which were subsequently developed by Dommain *et al.* (2010), who recommended that conservation and restoration efforts should take into account the interrelationships of vegetation, water and peat, along with the feedbacks that operate as a consequence. For example, rainfall is an important factor that affects soil moisture content, which in turn controls decomposition. Because peat in elevated situations (domes, hummocks, tussocks) is drier than that in topographical depressions (basins, hollows), it decomposes more readily and burns first (Belyea & Malmer 2004, di Folco & Kirkpatrick 2011) or erodes. The wetness of peat in depressions is controlled more by the substratum than by rainfall, and the presence of persistent standing water may limit the rate of peat accumulation by impeding primary production (Mäkilä & Moisanen 2007).

High resolution digital terrain models (DTMs) have been used in conjunction with soils data to robustly identify fine-scale geomorphic patterns in a subarctic landscape (Luoto & Hjort 2005); and to demonstrate strong positive correlation between rainfall, soil, relief and vegetation in humid environments (Sangireddy *et al.* 2016). Vernimmen *et al.* (2019) present a method for creating such DTMs for tropical peatlands using LiDAR data. LiDAR technology is able to measure objects on the land surface with a spatial resolution of 1–3 m and a minimum land surface height difference of 15 cm, making it highly suitable for the investigation of peatlands which generally exhibit rather flat morphology (Korpela *et al.* 2009, Bhardwaj *et al.* 2016, Simpson *et al.* 2016, Mackin *et al.* 2017, Korpela *et al*. 2020). On the other hand, information about peat thickness geometrically extracted from soil mapping data is unreliable with the potential to cause data repetition, because the thickness values are derived by extrapolation from sparsely distributed measurements. Thus, manual measurements of peat thickness are still necessary to obtain precise data on the diversity of substratum topography (Boehm *et al.* 2013, Young *et al.* 2018).

The objective of this study is to describe the relationships between peat characteristics (thickness and degree of decomposition) and the topography of both the ground surface and the substratum in tropical peat swamp on Tebing Tinggi Island off the east coast of Sumatra, Indonesia. We employ a mapping approach which combines the analysis of airborne LiDAR DTM and ground-based manual peat thickness measurements.
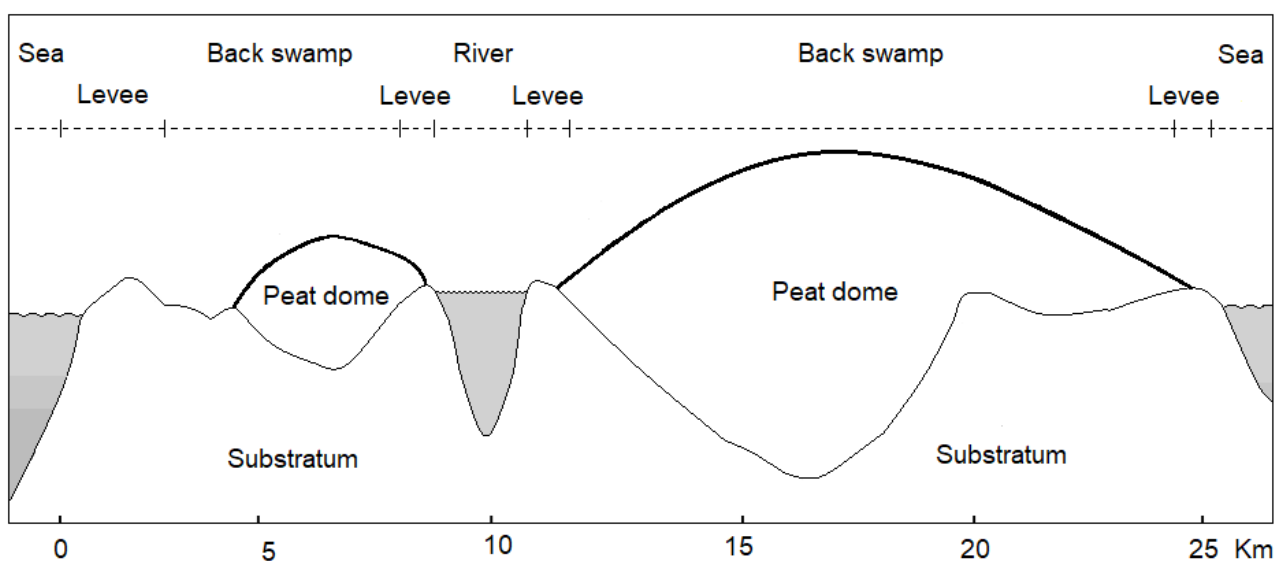

Figure 1. Diagrammatic cross-section of peat swamp morphology on Tebing Tinggi Island, showing the natural sequence of landforms: levées, back swamps and peat domes.

METHODS

Study location

The study was conducted on Tebing Tinggi Island (0° 41' 10"–1° 1' 20" N, 102° 24' 30"–103° 3' 25" E), Meranti Regency, Riau Province, Indonesia (Figure 2). The island (total area 1,436 km^2) is separated from the east coast of Sumatra by a strait which formed as a result of Holocene sea level rise (Dommain *et al*. 2011, Giesen *et al*. 2018), and is largely (90.45 %) covered by 1,299 km^2 of peatland. The subdued topography of Tebing Tinggi Island is typical of coastal peatlands in the tropics. Its surface altitude ranges from zero to 13.5 metres above sea level (m a.s.l.), averaging 6.98 m a.s.l. Tides are semidiurnal (Whitten *et al*. 2000) with amplitudes ranging from 1.42 m to 4.37 m (average 2.89 m) and the largest tides occurring over a period of 3–4 days annually.

The population of Tebing Tinggi Island at the 2010 census was 81,008. The main urban centre is Selat Panjang, around the port of Tanjung Harapan on the northern coast near the mouth of the Suir Kanan River. Other population centres include Sungai Tohor, Tanjung Mayau and Bengkikit around the coastline and Deremi in the interior. Local people have traditionally cultivated crops within the peat swamp forest. The sago palms of Tebing Tinggi Island are thought to be particularly rich in starch, which is nowadays exported to Java and Malaysia for processing into flour and other foods. Available estimates indicate that, in 2007–2010, ~ 570,000 t of mature sago logs were harvested and 100,000 t of dry starch produced annually by the numerous small-scale starch factories on the island, and the monthly production of sago paste (~ 500 t) by the community of Sungai Tohor had a commercial value of ~10,000 USD (Butler 2010, Smith 2015). Community-run farms additionally produce rubber (5,460 ha), coconut (3,740 ha), coffee (180 ha) and areca (70 ha). Sago is also grown by two private enterprises using semi-intensive cultivation systems (1,000–3,000 ha). Intensive planting of sago under a 20,000 ha government plantation licence started in 1996 and 12,000 ha had been planted by 2007 (Smith 2015). The licence for an adjacent industrial pulp and paper concession (recorded area 10,390 ha) was revoked under Decree of Ministry of Environment and Forestry Number 444/MENLHK/Setjen/HPL.I/6/2016. There is no planted oil palm anywhere on Tebing Tinggi.

The island has repeatedly experienced land fires during recent years as a result of dewatering of the peatland via extensive networks of drainage canals. A severe fire in 2015 affected 30 km^2 of the peatland, making Tebing Tinggi Island one of the highest-priority 'peatland hydrological units' for attention of the Indonesian Government's Peat Restoration Agency (BRG) (see, e.g., Tata 2019). The most recent
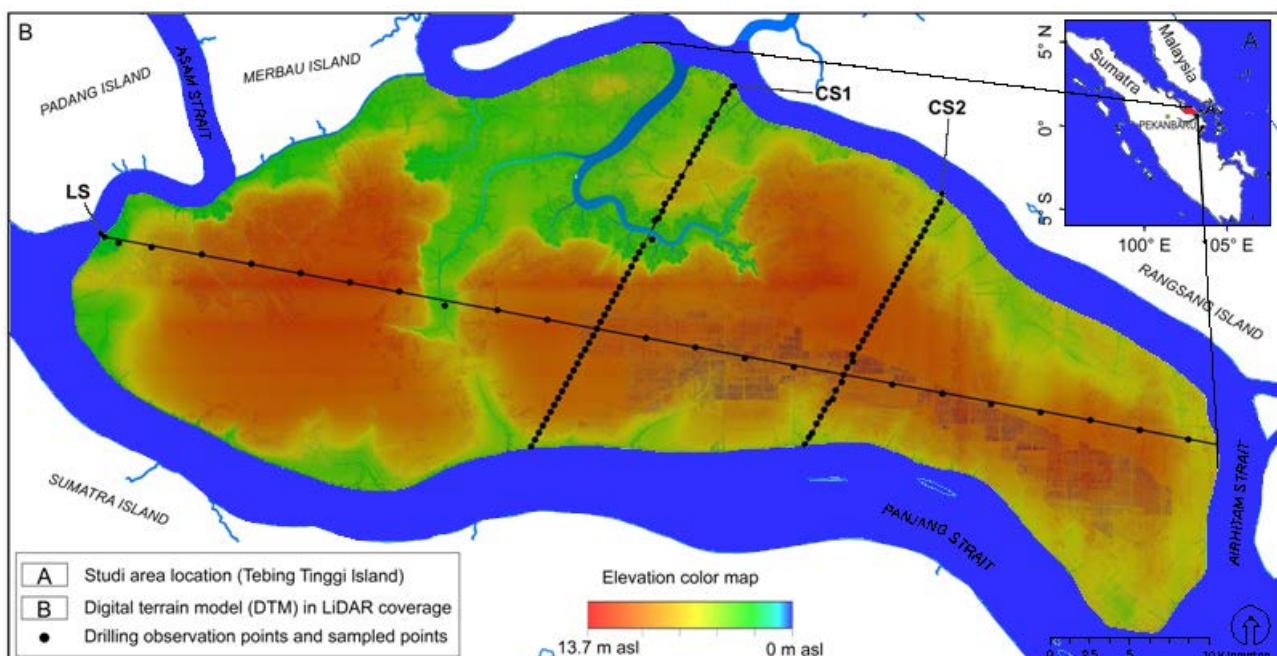

Figure 2. A (inset): the location of Tebing Tinggi Island in relation to Sumatra and peninsular Malaysia. B: the LiDAR coverage of Tebing Tinggi Island, shown as a digital terrain model (DTM; resolution 0.5 m) with our survey lines (LS, CS1, CS2) and plantation blocks of the sago concession (see outline in Figure 3) superposed.

fire on the island occurred in 2018 and burned across 1 km^2 of canalised peatland. Surviving peat swamp forest vegetation now covers only 28.34 % of the island, while the extent of shrub vegetation (indicative of fire-prone locations) has reached 21.20 % of the total area.

Digital terrain model (DTM)
The DTM (Figure 1) was developed using high density point cloud data without land cover, obtained using LiDAR technology. The acquisition of airborne LiDAR data was carried out by the Indonesian Ministry of Environment and Forestry between December 2016 and January 2017, recording with a frequency of four points per square metre. Subsequently, the data were processed with a spatial accuracy of < 10 cm. Ground truthing data points were measured to vertical (V) and horizontal (H) accuracies of V ≤ 4 cm and H ≤ 2 cm in November–December 2016 using a geodetic GPS receiver and static post-processing. We used the processed data as released by the Ministry of Environment.

Field and laboratory measurements
The field survey points were arranged along three transects crossing the island from coast to coast. Transect LS ('longitudinal section') was 69 km long with 24 survey points mostly spaced at 3 km intervals, running approximately west–east (WNW–ESE) along the long axis of the island; Transect CS1 ('cross section 1', perpendicular to LS) was 26 km long with 50 survey points at 500 m intervals; and Transect CS2 (15 km to the east of, and parallel to, Transect CS1) was 17.5 km long with 36 survey points at 500 m intervals. Land surface altitudes for the 110 survey points were derived from the LiDAR DTM using ArcGIS 10.3 software.

If peat was present at a survey point, its thickness was measured by 'drilling' with a peat corer (Eijkelkamp, Giesbeek, Netherlands) which extracts cores 50 cm long and 5.2 cm in diameter. At each coring location, cores were sequentially extracted from a single hole, from surface to substratum. Peat maturity was determined qualitatively by inspection in the field. A sample was squeezed in the palm of the hand and its maturity evaluated based on the remaining fibrous peat: > 75 % for fibric (immature), 25–75 % for hemic (medium), and < 25 % for sapric (mature) peat (Agus *et al.* 2011; Table 1). This information was used to distinguish different layers (I, II, III, IV) in the peat profile. Samples for laboratory analysis were collected from each peat layer in 12 of the cores (five from Transect LS, four from Transect CS1 and three from Transect CS2; see next paragraph). Finally, the pyrite content of the substratum was determined by the H_2O_2 test (Utami *et al.* 2014).

Twelve cores were selected to represent three different peat thickness groups (< 3 m, 3–6 m and > 6 m) between which we noted differences in character of the peat. One undisturbed and one disturbed peat sample was taken from each peat layer in these cores. Undisturbed peat samples were taken using a metal ring with a volume of 100 cm^3. These samples were used for laboratory determination of bulk density, water content and ash content using standard methods for peat (Jarrett 1983, Radjagukguk *et al.* 2000, Agus *et al.* 2011). In total, 29 undisturbed peat samples were oven dried at 105 °C with daily weighing for two days (48 h), after which they were found to have reached constant weight, enabling the calculation of bulk density and water content. Ash content was determined for 29 disturbed dry peat samples (5 g) by ashing in a muffle furnace at 700 °C for five hours.

Table 1. The simplified field method for determination of 'peat maturity' derived for Indonesian peatlands, after Agus *et al.* (2011).

Maturity class	Description
Fibric (immature)	Peat at early stage of decomposition with original materials still recognisable, brown to light brown in colour and, when squeezed in the palm, more than two-thirds of its original amount remains in hand.
Hemic (medium)	Half-decomposed peat with some of the original materials still recognisable, brown in colour and when squeezed in the palm between one-third and two-thirds of the original amount remains.
Sapric (mature)	Advanced stage of decomposition with original materials not recognisable, dark brown to black in colour and when squeezed in the palm less than one-third of the original amount remains.

Statistical analysis

Peat thickness was zero at 16 of the 110 survey points (3 on LS, 10 on CS1 and 3 on CS2), and these were removed from the dataset before further analysis. For each of the remaining 94 survey points, peat thickness was subtracted from land surface altitude to obtain substratum altitude. The relationships between land surface altitude, peat thickness and substratum altitude were then examined using simple linear regression models and Pearson correlation. The first two linear regressions were carried out with land surface altitude as the independent variable, peat thickness and substratum altitude as dependent variables. The 5 % confidence value (P-value) was used to assess the significance of the relationships; if P-value < 5 % there was a significant correlation between the paired variables, and if P-value > 5 % there was no significant correlation. All statistical analysis was conducted in SPSS 23 for Windows.

RESULTS

Profiles of topography and peat thickness

Figure 3 shows surface contours of Tebing Tinggi Island (derived from the DTM) with the survey lines (transects) and coring locations superposed, and Figures 4–6 show profiles along the three transects.

Transect LS crosses two peat domes separated by the Suir Kanan River, presenting in vertical section (Figure 4) a lower and flatter profile for the eastern dome (average surface altitude 8.84 m a.s.l.) than for the western one (average surface altitude 9.11 m a.s.l.). Starting from the natural levée at the western coast of the island (Point 2), the examined profile of the western dome rises by 9.00 m across a distance of 15 km to a summit (Point 7) 6 km west of the Suir Kanan River. The highest point recorded on the eastern dome (Point 19) lies 30 km from the river, 6.70 m higher than the river, and 15 km from the back swamp on the eastern coast of the island (Point 24). Measured peat thickness in the western peat dome is up to 12.10 m (mean = 7.61 m), while in the eastern dome it is up to 10.25 m (mean = 5.90 m). Where land surface height (a.s.l.) exceeds peat thickness, the substratum forms mounds beneath the peat (Points 3, 5, 8, 11, 16, 18 and 22 in Figure 4). On the other hand, where the land surface height a.s.l. is less than peat thickness, the peat overlies basins in the substratum (Points 4, 6, 13, 17, 20 and 23 in Figure 4).

Transect CS1 also crosses two peat domes (Figure 5). Along this profile, the average land surface heights for the northern and southern peat domes are 5.14 m and 7.97 m a.s.l., respectively. The highest point recorded on the northern dome (Point 11) is 3 km distant from and 3.50 m higher than the back swamp (Point 5), and 4 km from the Suir Kiri River (Point 19); while the southern dome transect rises to 6.20 m above the back swamp at Point 5 within a distance of 3 km from the river
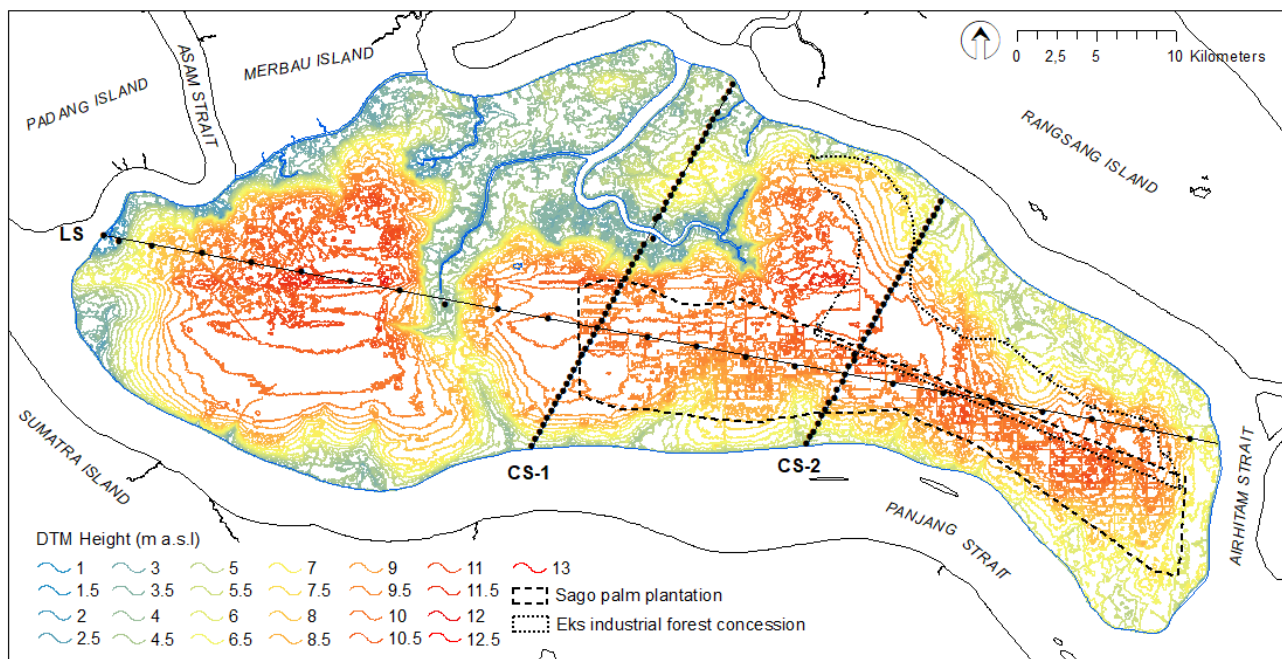

Figure 3. Contour map of Tebing Tinggi Island derived from the DTM shown in Figure 2, with the three survey transects (LS, CS1 and CS2) and outlines of industrial plantation areas superposed.
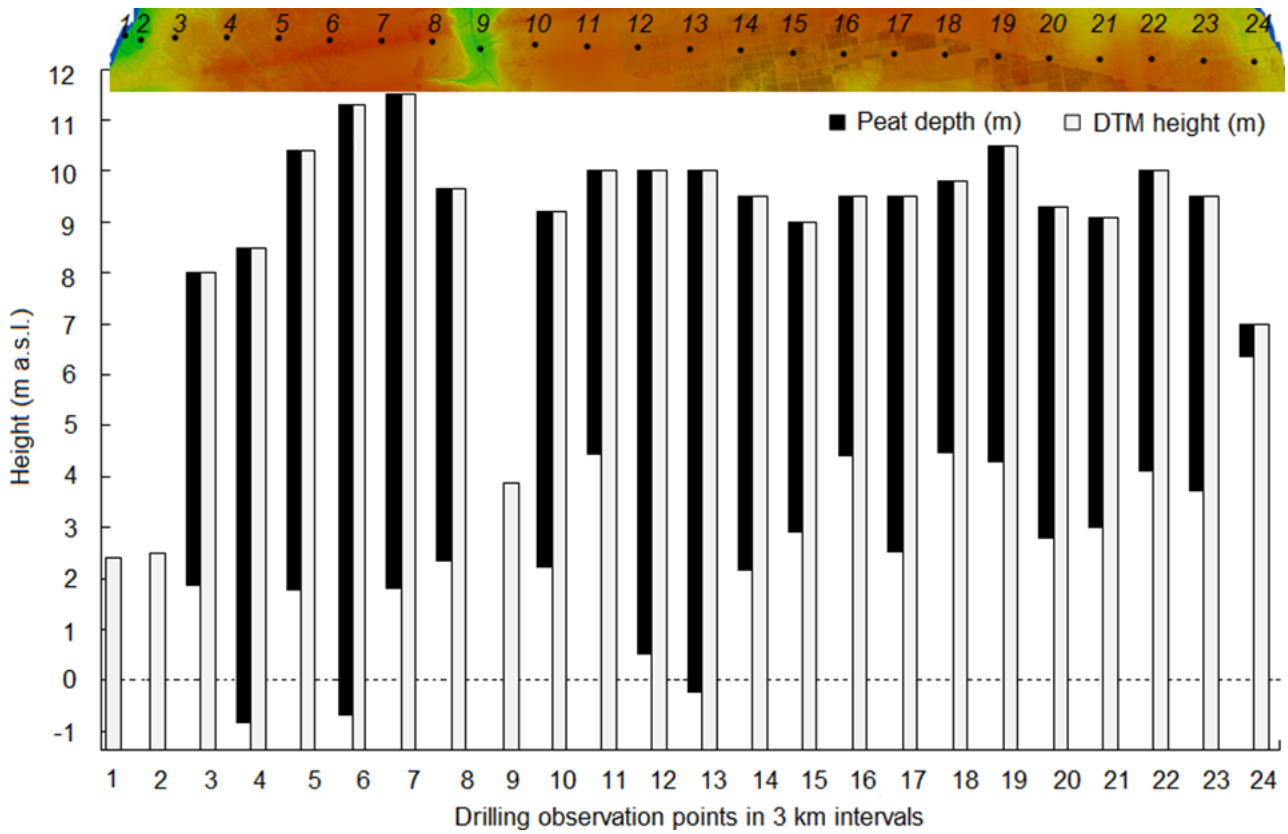
Figure 4. Longitudinal section from west (left-hand side of diagram) to east along Transect LS. Above the profile, the plan locations and numbering of survey points are superposed on a strip of the DTM shown in Figure 2.
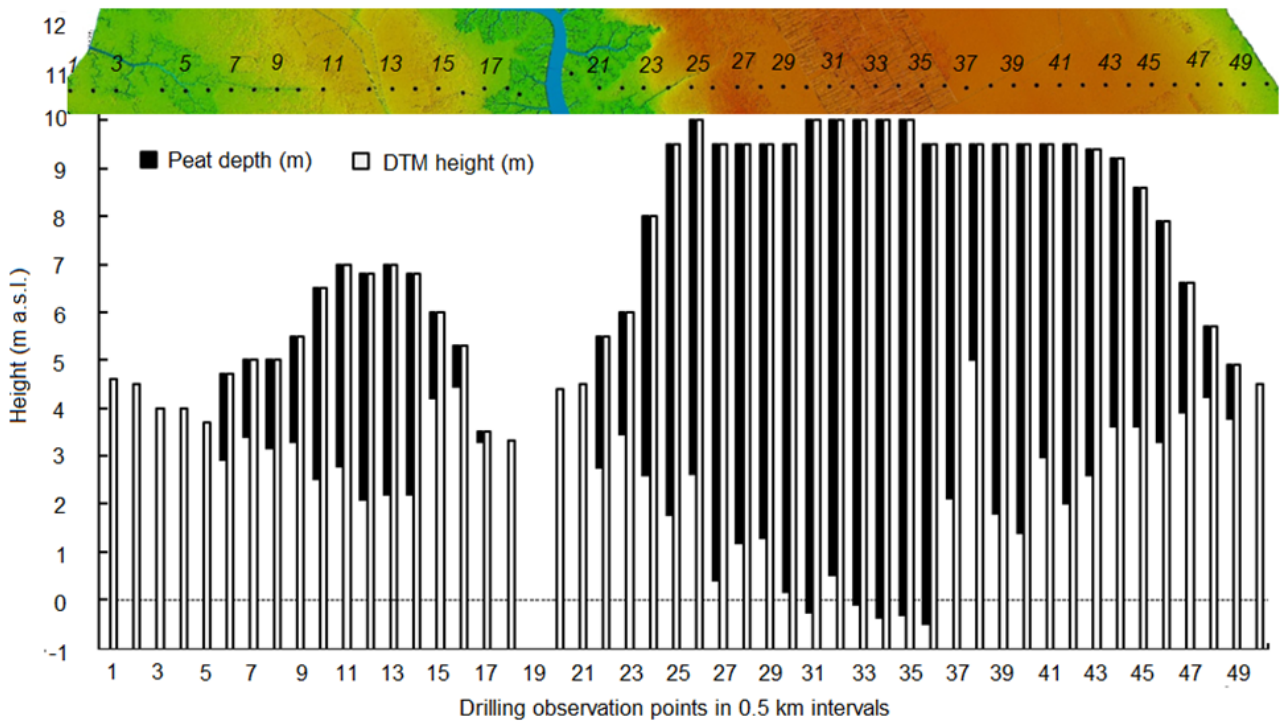

Figure 5. Longitudinal section from north (left-hand side of diagram) to south along Transect CS1. Above the profile, the plan locations and numbering of survey points are superposed on a strip of the DTM shown in Figure 2.

(at Point 25, which is 12.5 km from the natural levée at Point 50 on the southern coast of the island). The summit of the southern peat dome is flattened over a distance of 8.5 km (Points 25 to 42), with 12 of the surveyed points lying at altitude 9.5 m a.s.l. and six at 10 m a.s.l. Mean peat thickness in the northern peat dome is 1.71 m (maximum = 4.80 m), and in the southern peat dome 5.77 m (maximum = 10.40 m). Where the land surface height is greater than the thickness of the peat, the substratum again forms mounds beneath the peat (Points 7, 16, 23, 26, 29, 32, 38, 41, 44 and 48 in Figure 5). Conversely, where land surface heights are lower than the peat thickness, there are basins in the substratum at the base of the peat (Points 12, 27, 31, 36, 40, 42 and 46).

In Transect CS2 (Figure 6), Points 1 and 34–36 are located on natural levées not affected by tides, but coastal abrasion due to scouring by sea waves has penetrated 1 m into the transect. At the northern end of this transect, a zone of coastal peat can be demarcated from the main dome at Point 5. Here, seawater penetration (indicated by the presence of mangroves) reaches 650 m from the coastline, while around natural levées and drainage canals it can reach 1–3 km. Although peat is not present in areas with direct tidal influence, local communities have planted sago on shallow peat adjacent to the mangrove zone, causing the coastal peat to be different from that inland. For Transect CS2, the average land surface height is 8.44 m a.s.l.; the difference between the

highest and lowest points on the main dome is 5.00 m; and the highest surface point recorded lies 6.5 km from Point 5 and 9 km from the southern coast of the island. Peat thickness (up to 8.70 m; mean = 5.85 m) varies, but not in accordance with surface altitude. Where surface altitude exceeds peat thickness, the substrate forms mounds beneath the peat (Points 2, 8, 14, 20, 22, 28, 32 in Figure 6). Conversely, locations where surface altitude is less than peat thickness (e.g. Points 4, 9, 16, 21, 25, 29) reflect the presence of basins in the substratum.

Statistical analysis of topography and peat thickness

The results of the statistical analysis are shown in Figure 7. For the western and eastern domes of Transect LS, surface altitude shows a significant correlation with peat thickness ($R^2 = 0.46$; P-value = 0.001) but no correlation with substratum altitude ($R^2 = 0.11$; P-value = 0.15). Substratum altitude also shows a significant correlation with peat thickness ($R^2 = 0.84$; P-value < 0.001). For the northern and southern peat domes of Transect CS1, surface altitude shows significant correlations with both peat thickness ($R^2 = 0.87$; P-value < 0.001) and substratum altitude ($R^2 = 0.40$; P-value < 0.001). Substratum altitude shows a significant correlation with peat thickness ($R^2 = 0.76$; P-value < 0.001). For Transect CS2, the surface height of the peat dome shows a significant correlation with peat thickness ($R^2 = 0.74$;
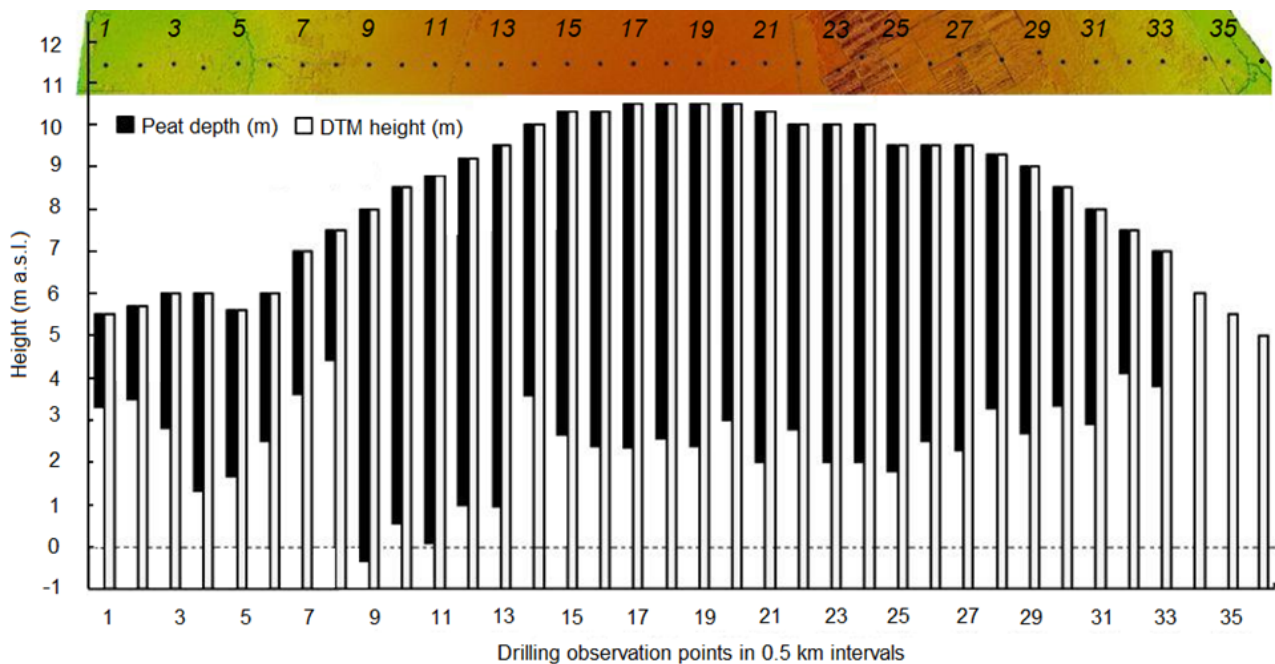
Figure 6. Longitudinal section from north (left-hand side of diagram) to south along Transect CS2. Above the profile, the plan locations and numbering of survey points are superposed on a strip of the DTM shown in Figure 2.
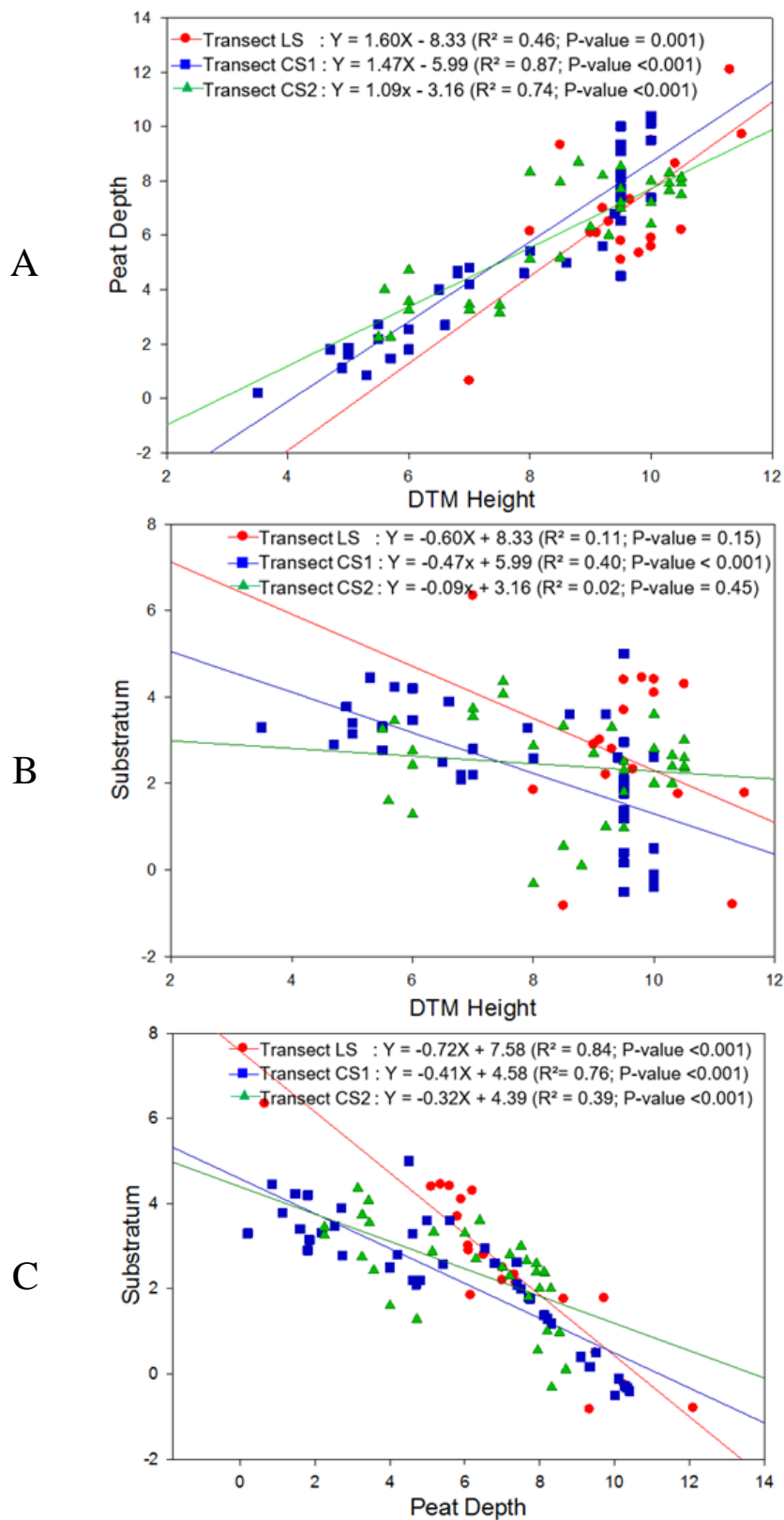
Figure 7. Linear regression relationships between land surface altitude (DTM height), peat thickness (= peat depth) and substratum altitude. All relationships between DTM height and peat depth (Panel A), and between substratum altitude and peat depth (Panel C) are significant (P-value < 0.05), but there is no significant relationship (P-value > 0.05) between DTM height and substratum altitude (Panel B) in Transects LS and CS2. Number of observations (n) is 21 for Transect LS, 40 for Transect CS1 and 33 for Transect CS2.

P-value < 0.001) but no correlation with substratum altitude (R^2 = 0.02; P-value = 0.45). Substratum altitude shows a significant correlation with peat thickness (R^2 = 0.39; P-value < 0.001).

Characteristics of peat and mineral substratum
Results characterising the peat layers and mineral substratum based on cores from the 12 representative survey points are summarised in Table 2, and the full results are provided in Table A1 in the Appendix.

Layer I consists of hemic and, especially around drainage canals, slightly sapric material. Layer II is composed of fibric and hemic material, while Layers III and IV are consistently composed of fibric material. Water content is higher in the deeper layers, i.e. Layers III and IV, which can be linked to the greater concentration of fibric material in these layers because saturation is thought to inhibit the decomposition process. Bulk density ranges from 0.09 to 0.26 g cm^{-3} and averages 0.17 g cm^{-3}. In the thinnest peat category (< 3 m), bulk density is higher (i.e. the peat is more compact) in Layer I than in Layers II and III, and this variation in compactness can be related to degree of decomposition, the upper layer (I) being more decomposed (sapric/hemic) than the lower layers (hemic/fibric).

Ash content ranges from 0.15 % to 4.67 % (average 2.07 %), indicating highly lignitic acid peat of the low-fertility oligotrophic type. The very high ash content at Point CS1_13 could be due to mixing of peat and mineral materials at the bottom of the profile during coring.

The substratum is dominated by clay sediments containing sulfidic/pyrite material, which is characterised by a weak to strong H_2O_2 reaction, a pH of 1.5–3.5 and a bluish-grey colour.

Table 2. Characterisation of peat thickness and mineral substratum at 12 selected survey points on Transects LS, CS1 and CS2.

Peat depth class and selected survey points	Peat layer	Peat thickness (m)			Peat maturity	Bulk density (g cm^{-3})	Water content (% of wet weight)	Ash content (%)	Sub-stratum
		min	max	mean					
< 3 m: LS_23 CS1_48 CS1_17 CS2_5	I	0.07	0.68	0.33	sapric, hemic	0.24	76.16	1.56	clay, silt
	II	0.29	2.77	1.04	hemic, fibric	0.16	88.18	1.98	
	III	1.37	1.37	1.37	fibric	0.17	87.16	2.57	
3–6 m: LS_20 CS1_13 CS2_11	I	0.29	0.74	0.55	sapric, hemic	0.15	82.05	2.05	clay, silt, silty clay
	II	0.49	4.36	1.78	hemic, fibric	0.15	87.85	2.94	
	III	3.21	3.83	3.52	fibric	0.21	86.62	2.80	
	IV	0.19	0.19	0.19	fibric	0.14	89.20	4.67	
> 6 m: LS_4 LS_7 LS_13 CS1_35 CS2_19	I	0.15	0.62	0.37	sapric, hemic	0.15	86.63	1.40	clay, silt, silty clay
	II	0.54	9.14	4.81	hemic, fibric	0.14	88.94	2.05	
	III	5.41	5.59	5.50	fibric	0.15	88.21	1.19	

DISCUSSION

This study has demonstrated the potential, as well as some pitfalls, of using of LiDAR DTM data in conjunction with ground-based peat coring for investigation of the distribution and thickness of peat deposits and the topographical characteristics of the substratum, in this instance on Tebing Tinggi Island. We found no consistent relationship between the surface topography of the island and peat thickness, i.e. the three-dimensional shape of the peat deposit is not directly related to the topography of the substratum, whose altitude may vary over short distances. For example, at Points 36 and 37 on Transect CS1 (Figure 5) and at Points 9 and 8 on Transect CS2 (Figure 6), where the base of the peat layer is in the valley of an ancient riverbed and on a natural levée, respectively, the difference in peat thickness between observation points only 500 m apart is more than 2 m. A practical consequence is that it is difficult to accurately replicate measurements of peat thickness, even in adjacent locations or at relocated geographical coordinates. Also, measurements taken at different times and/or by different personnel may vary because there is a subjective element in identification of the base of the peat layer. Nonetheless, the coring data collected, in conjunction with the surface topography derived from LiDAR, provide wide-ranging insights about the Tebing Tinggi peat deposit.

The three-dimensional form of a peat dome may depend on: the influence of the sea, rivers and mineral geology (Maas 2014); the historical duration of peat formation (Hodgkins *et al.* 2018) which may in turn be determined by fluctuations on geological timescales in the levels of rivers and the sea as well as by climate change; and it may also be affected by human activities (Hapsari *et al.* 2018), which may have implications for peatland functions such as water and carbon storage. We consider our findings in the context of some of these influences below.

The surface topography of the peat-covered landscape surveyed in this study consists of convex (dome) and concave (basin) surfaces. The peat layer is generally thicker in domes, which are ombrogenous (i.e. receive water only as rainfall from above), than in basins (Figures 4–6). The spatial pattern of domes and basins creates a high diversity of surface wetness. However, the volume of water discharged from a peatland is highly dependent on the groundwater level and hydraulic gradients in peat domes (Lampela *et al.* 2016). At Survey Points CS2_6–18 (Figure 6), runoff from the peat dome forms a natural channel that widens downstream as it approaches the sea. Such creeks slope more steeply

than the rivers into which they discharge and have not formed natural levées. Due to their steepness they can be expected to promote the outflow of water from the peat dome. From the profile shown in Figure 4, water outflow would be similarly enhanced on both sides of the Suir Kanan River where Transect LS crosses its headwaters; and owing to the greater altitude of the summit of the western dome, reached over a similar distance, the effect would be greater for that dome than for the eastern one, with implications for peat erosion.

At Survey Points CS1_27–42 (Figure 5) and CS2_22–30 (Figure 6) there is evidence that human activities have influenced the relief of the peatland surface, which is flattened within the sago plantation. The blocks of planted sago are equipped with canals that cut through the peat dome in a regular pattern, generally with small canals within the plantation and wider ones running parallel to the road at the edge of the plantation. The canals are lower-lying than the planted areas and, therefore, receive runoff water from the plantation. After rainfall, the runoff water often causes small scours in the soft organic peat material at the edge of the plantation.

The results from this study demonstrate that the surface altitude of the peatland has no consistent relationship with peat thickness. The combination of these two measurements gives different and variable land surface configurations. The DTM shows that the highest land is in the central part of the island and the lowest-lying land is near the coastline. However, the thickest peat does not necessarily underlie the most elevated land surfaces; thicker peat may have accumulated over a valley in the substratum near the edge of the island, while thinner peat may be found overlying mounds in the substratum farther inland. In other words, the surface altitude of the peatland is not related to substratum altitude, nor does the surface relief reflect substratum topography. The surface of the peatland takes the form of relatively smooth domes, whereas the relief of the underlying mineral layer ranges from gently to quite abruptly undulating (Figures 4–6), and correlations between the altitudes of peat surface and substratum are weak or absent (Figure 7A). Figures 4–6 show the contrast in topographical character between the undulating surface of the substratum and the more gently doming upper surface of the peat layer along our three transects.

The distance from the edge of the peat dome to the coast varies from 3 km to 10 km. In coastal areas, the accumulation of peat is limited by the extent to which sea water penetrates inland. Inundation of the substratum by sea water limits lateral extension of the peat layer through the deposition of fine fluvial

sediments, thus blocking outward expansion of the perched (fresh) water table (Gastaldo 2010). Sea water has the ability to act as an agent of sediment deposition that is able to penetrate upstream through tidal channels (Leonardi *et al.* 2018). Penetration of sea water causes depletion of groundwater which further increases the rate of decay of organic matter (Walter *et al.* 2018). Thus, the relatively small land area of Tebing Tinggi Island can be expected to decrease every year under the current trend of rising sea level.

The decline in sea level that occurred during the Ice Age (26,500–19,000 BP) caused intense erosion in the upper catchments of tropical rivers. Coarse materials such as gravel were deposited on tertiary sediments in the valleys downstream (Bird *et al.* 2005). When the ice retreated, sea level was 123 m lower than it is today and the islands of Sumatra, Borneo (including Kalimantan), Java and Bali were a single landmass connected with mainland Asia, forming the Sunda Shelf (Hanebuth *et al.* 2009). At that time the Malacca Strait (between the east coast of Sumatra and the west coast of peninsular Malaysia; see Figure 2 inset) was a gently sloping open valley. There were current-scoured swales as deep as 40 m on the exposed sea floor which then became rivers that extended to form the major Pleistocene river systems (Hanebuth *et al.* 2011, Voris 2017). These large rivers had their own catchment boundaries (Post *et al.* 2013). One of them was the 'Malacca River', whose catchment was bordered by the Bukit Barisan Mountains (western Sumatra) in the west, Tanjung Balai Karimun and Batam in the south and the Malaysian Titiwangsa Mountains to the east. The Malacca River drained northwards into the Andaman Sea. The Panjang, Padang and Air Hitam Straits of today (see Figure 1) are thought to have formed from channels of this ancient river system that drained a high plateau within the catchment, of which Tebing Tinggi and the other islands nearby are the only parts that still lie above sea level.

The process of organic matter accumulation that resulted in the formation of peatlands began in the early stages of the Holocene period (10,000–5,000 BP), coincident with rising sea levels (transgression) (Phys *et al.* 2000, Wu & Bustin 2004, Hanebuth *et al.* 2011). At that time, the entire east coast of Sumatra was already inundated by sea water. A rapid rise in sea level occurred between 19,000 and 7,000 BP (Dommain *et al.* 2014) and was accompanied by an increase in temperature and rainfall which caused strong chemical weathering of rocks in the Bukit Barisan mountains that resulted in the deposition of fine clay along the eastern coastline of Sumatra,

including across our research area. Processes of coastal plain formation and shifting of shorelines occurred gradually under the agency of water flows with different intensities and were followed by peat formation. Previously, the continuous submersion of the ancient river valleys had prevented the development of coastal peat, and it was only when the rate of sea level rise started to decline that the accumulation of coastal peat domes could begin (Dommain *et al.* 2014). The maximum initiation and expansion of peatland along the east coast of Sumatra occurred between 7,000 and 4,000 BP, when the sea level became more stable and similar to that of today (Sabiham & Basuki 1989). Available estimates of the age of peat carbon at the base of the peat layer are 4740–5730 years on Bengkalis Island and 3620–5220 years around the Siak Kanan River (Supardi *et al.* 1993), but there is currently no information about the age of the peat deposits on Tebing Tinggi Island. The peatland on the east coast of Sumatra formed directly on former seabed, as indicated by the presence of pyrite and seashells as well as the lack of mangrove remains in mineral sediments beneath the peat (Diemont & Supardi 1987, Sorensen 1993). For the most recent expansion of coastal peatland formation around the Sunda Shelf, which took place over the last two millennia (2,300–200 BP), radiocarbon evidence has shown that newly exposed coastal sediments were rapidly covered by layers of peat (Dommain *et al.* 2011), and on this basis we surmise that marshes which formed during the early Holocene period of coastline extension were replaced by swamp plants such as nipa palm and mangroves, followed by peat swamp forest plants. The original fluvial depositional environment (part of the river channel) turned into a paralic one (separated from the river by a levée) where freshwater plants and animals began to establish and dead trees and ferns partially decomposed with the help of anaerobic bacteria, augmented occasionally by aerobic bacteria during the dry season, to become peat deposits (Kool *et al.* 2006).

The data we present here are consistent with the notion that this rapid peat formation has preserved, uneroded, a young sedimentary landscape as it was some 3,000–5,000 years ago, in much the same way as was recently reported for palaeochannels of the San River in the Polish Carpathians by Kukulak & Szubert (2020). This arises as a consequence of the difference in geological and parent materials between the mineral substratum and the peat layer.

To aid in interpretation of the palaeo-landscape of Tebing Tinggi, Figure 8 shows conceptualisations of the three surveyed profiles of surface and substratum relief, as well as our information about the peat
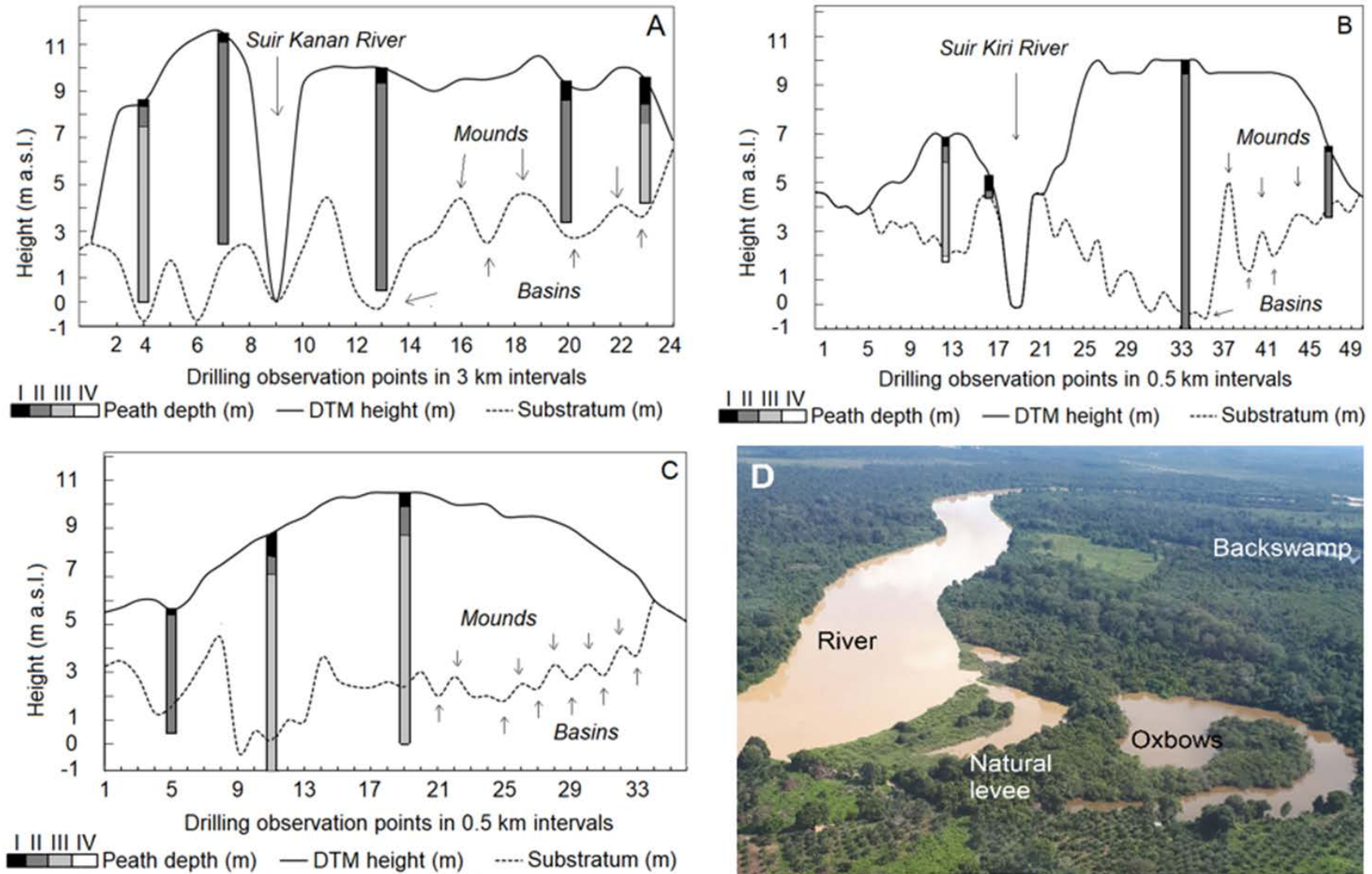
Figure 8. Conceptualised profiles of surface and substratum topography along the three surveyed transects on Tebing Tinggi Island (A: Transect LS; B: Transect CS1; C: Transect CS2), also showing the locations and peat layers (I –IV) of the twelve cores selected for laboratory examination; and (D) visualisation of river morphology in the form of natural levées, meanders, oxbow lakes and backswamp. Photo: Azwar Maas.

layers, alongside an oblique aerial image of a lower reach of the river. The sedimentation capacity of fluvial systems is determined by the slope of the floodplain and the peak surface runoff (Notebaert *et al.* 2010). The low-gradient segment of the ancient Malacca River illustrated offers a depositional environment for its heavy load of sediment, which continuously settles on the natural levées whence it is absorbed into the back swamp or, at low flows, settles directly on the riverbed (Eekhout *et al.* 2015). Physically, the river is characterised by meanders and oxbow formations (Figure 8D). Owing to river morpho-dynamic processes, the meanders will continuously evolve and it is therefore common to find oxbows arranged in series to achieve flow balance. This causes an irregular unevenness of the ground by introducing a random pattern of mounds and intervening depressions (basins and/or valleys) which is well matched to the apparent topography of the substratum located beneath the peat layer in all three of our transects (Figures 8A–8C).

Given the lack of basic geological information for Tebing Tinggi Island (for example, no map of Quaternary sediments is currently available), morphological studies such as the one described here have potential to provide clues about early Holocene environmental changes and sediment dynamics on floodplains and alluvium plains, which can be linked to the evolution of the ancient river channels and valleys in this study region. Our data also provide a striking indication of the difference in character of the island's surface relief between the present day and the time prior to peat formation, or in a future scenario after disappearance of the peat layer due to excessive subsidence. Especially worthy of note is the fact that there are locations on all of our transects which, in the absence of peat, would now lie below sea level.

ACKNOWLEDGEMENTS

AUTHOR CONTRIBUTIONS

All authors conceived the study and this article. BN was responsible for processing of the LiDAR DTM, data analysis, manuscript writing, addressing reviewers' comments and revising the manuscript. AM coordinated the BRG researchers, acquired the LiDAR DTM data, and was directly involved in the research design and discussion of results. SNHU guided laboratory measurements for peat characteristics, responded to reviewers' comments and revised the manuscript. MN guided the field measurements for topographic profiles and peat thickness, and provided inputs for revisions.

REFERENCES

Agus, F., Hairiah, K., Mulyani, A. (2011) *Measuring Carbon Stock in Peat Soils: Practical Guidelines*. World Agroforestry Centre (ICRAF) Southeast Asia Regional Program, Indonesian Centre for Agricultural Land Resources Research and Development, Bogor, Indonesia, 60 pp. Online at: http://old.worldagroforestry.org/downloads/Publications/PDFS/MN17335.PDF

Belyea, L.R., Malmer, N. (2004) Carbon sequestration in peatland: patterns and mechanisms of response to climate change. *Global Change Biology*, 10(7), 1043–1052.

Bhardwaj, A., Samb, L., Bhardwaj, A., Martín-Torres, F.J. (2016) LiDAR remote sensing of the cryosphere: Present applications and future prospects. *Remote Sensing of Environment*, 177, 125–143.

Bird, M.I., Taylor, D., Hunt, C. (2005) Palaeoenvironments of insular Southeast Asia during the last glacial period: a savanna corridor in Sundaland? *Quaternary Science Reviews*, 24, 2228–2242.

Boehm, H.V., Liesenberg, V., Limin, S.H. (2013) Multi-temporal airborne LiDAR-survey and field measurements of tropical peat swamp forest to monitor changes. *IEEE Journal of Selected Topics in Applied Earth Observations and Remote Sensing*, 6(3), 1524–1530.

Bragg, O.M. (1997) Understanding ombrogenous mires of the temperate zone and the tropics: an ecohydrologist's viewpoint. In: Rieley, J.O., Page, S.E. (eds.) *Biodiversity and Sustainability of Tropical Peatlands*, Samara Publishing, Cardigan, UK, 135–146.

Butler, R.A. (2010) Logging may swamp Indonesian peatlands, destroy local sustainable sago industry. *Mongabay*. Online at: https://news.mongabay.

com/2010/08/logging-may-swamp-indonesian-peatlands-destroy-local-sustainable-sago-industry/, accessed 04 Jun 2020.

Couwenberg, J., Hooijer, A. (2013) Towards robust subsidence-based soil carbon emission factors for peat soils in south-east Asia, with special reference to oil palm plantations. *Mires and Peat*, 12, 01, 13 pp.

Diemont, H., Supardi, H. (1987) Forest peat in Indonesia on former sea beds. In: *International Peat Society Symposium on Tropical Peat and Peatlands for Development, Yogyakarta, Indonesia, February 9–14, Abstracts*, 709–717.

di Folco, M.-B., Kirkpatrick, J.B. (2011) Topographic variation in burning-induced loss of carbon from organic soils in Tasmanian moorlands. *Catena*, 87(2), 216–225.

Dommain, R., Couwenberg, J., Joosten, H. (2010) Hydrological self-regulation of domed peatlands in south-east Asia and consequences for conservation and restoration. *Mires and Peat*, 6, 05, 17 pp.

Dommain, R., Couwenberg, J., Joosten, H. (2011) Development and carbon sequestration of tropical peat domes in south-east Asia: links to post-glacial sea-level changes and Holocene climate variability. *Quaternary Science Reviews*, 30(7–8), 999–1010.

Dommain, R., Couwenberg, J., Glaser, P.H., Joosten, H., Suryadiputra, I.N.N. (2014) Carbon storage and release in Indonesian peatlands since the last deglaciation. *Quaternary Science Reviews*, 97, 1–32.

Eekhout, J.P.C., Hoitink, A.J.F., Brouwer, J.H.F.D., Verdonschot, P.F.M. (2015) Morphological assessment of reconstructed lowland streams in the Netherlands. *Advances in Water Resources*, 81, 161–171.

Gastaldo, R.A. (2010) Peat or no peat: Why do the Rajang and Mahakam Deltas differ? *Coal Geology*, 83(2–3), 162–172.

Giesen, W., Wijedasa, L.S., Page, S.E. (2018) Unique Southeast Asian peat swamp forest habits have relatively few distinctive plant species. *Mires and Peat*, 22, 01, 13 pp.

Graniero, P.A., Price, J.S. (1999) The importance of topographic factors on the distribution of bog and heath in a Newfoundland blanket bog complex. *Catena*, 36(3), 233–254.

Hanebuth, T.J.J., Stattegger, K., Bojanowski, A. (2009) Termination of the last glacial maximum sea-level lowstand: The Sunda-Shelf data revisited. *Global and Planetary Change*, 66(1–2), 76–84.

Hanebuth, T.J.J., Voris, H.K., Yokoyama, Y., Saito, Y. (2011) Formation and fate of sedimentary depocentres on Southeast Asia's Sunda Shelf over the past sea-level cycle and biogeographic implications. *Earth Science Reviews*, 104(1–3), 92–110.

Hapsari, K.A., Biagioni, S., Jennerjahn, T.C., Reimer, P., Saad, A., Sabiham, S., Behling, H. (2018) Resilience of a peatland in Central Sumatra, Indonesia to past anthropogenic disturbance: Improving conservation and restoration designs using palaeoecology. *Journal of Ecology*, 1–18.

Harrison, M.E., Rieley, J.O. (2018) Tropical peatland biodiversity and conservation in Southeast Asia: Foreword. *Mires and Peat*, 22, 00, 7 pp.

Hirano, T., Segah, H., Kusin, K., Limin, S. (2012) Effects of disturbances on the carbon balance of tropical peat swamp forests. *Global Change Biology*, 18, 3410–3422.

Hodgkins, S.B., Richardson, C.J., Dommain, R., Wang, H., Glaser, P.H., Verbeke, B., Winkler, B.R., Cobb, A.R., Rich, V.I., Missilmani, M., Flanagan, N., Ho, M., Hoyt, A.M., Harvey, C.F., Vining, S.R., Hough, M.A., Moore, T.R., Richard, P.J.H., De La Cruz, F.B., Toufaily, J., Hamdan, R., Cooper, W.T., Chanton, J.P. (2018) Tropical peatland carbon storage linked to global latitudinal trends in peat recalcitrance. *Nature Communications*, 9, 3640, 13 pp.

Hooijer, A., Page, S., Jauhiainen, J., Lee, W.A., Lu, X.X., Idris, A., Anshari, G. (2012) Subsidence and carbon loss in drained tropical peatlands. *Biogeosciences*, 9, 1053–1071.

Jaenicke, J., Rieley, J.O., Mott, C., Kimman, P., Siegert, F. (2008) Determination of the amount of carbon stored in Indonesian peatlands. *Geoderma*, 147, 151–158.

Jarrett, P.M. (1983) *Testing of Peats and Organic Soils*. Special Technical Publication 820, ASTM International, West Conshohocken PA, 218–239.

Kool, D.M., Buurman, P., Hoekman, D.H. (2006) Oxidation and compaction of a collapsed peat dome in Central Kalimantan. *Geoderma*, 137(1–2), 217–225.

Korpela, I., Koskinen, M., Vasander, H., Holopainen, M., Minkkinen, K. (2009) Airborne small-footprint discrete-return LiDAR data in the assessment of boreal mire surface patterns, vegetation, and habitats. *Forest Ecology and Management*, 258, 1549–1566.

Korpela, I., Haapanen, R., Korrensalo, A., Tuittila, E.-S., Vesala, T. (2020) Fine-resolution mapping of microforms of a boreal bog using aerial images and waveform-recording LiDAR. *Mires and Peat*, 26, 03, 24 pp.

Kukulak, J., Szubert, M. (2020) Substratum sedimentology and topography of two riparian peat bogs in the Bieszczady Mountains (Carpathians). *Mires and Peat*, 26, 12, 13 pp.

Laamrani, A., Valeria, O., Bergeron, Y., Fenton, N., Cheng, L.Z., Anyomi, K. (2014) Effects of topography and thickness of organic layer on productivity of black spruce boreal forests of the Canadian clay belt region. *Forest Ecology and Management*, 330, 144–157.

Lampela, M., Jauhiainen, J., Kämäri, I., Koskinen, M., Tanhuanpää, T. (2016) Ground surface microtopography and vegetation patterns in a tropical peat swamp forest. *Catena*, 139, 127–136.

Leonardi, N., Carnacina, I., Donatelli, C., Kamal, N., James, A., Schuerch, M., Temmerman, S. (2018) Dynamic interactions between coastal storms and salt marshes: a review. *Geomorphology*, 301, 92–107.

Luoto, M., Hjort, J. (2005) Evaluation of current statistical approaches for predictive geomorphological mapping. *Geomorphology*, 67, 299–315.

Maas, A. (2003) *Pidato Pengukuhan: Peluang dan Konsekuensi Pemanfaatan Lahan Rawa Pada Masa Mendatang* (*Opportunities and Consequences of Using Swampland in the Future*). Inaugural Speech of Professorship at the Faculty of Agriculture, Universitas Gadjah Mada, Yogyakarta, 17 pp. (in Indonesian).

Maas, A. (2014) Lahan pertanian di lahan rawa (Farmland in swampland). In: Maas, A. (ed.) *Pengelolaan Lahan Rawa untuk Pertanian* (*Management of Swampland for Agriculture*), Faculty of Agriculture, Universitas Gadjah Mada, Yogyakarta, 1–27 (in Indonesian).

Mackin, F., Flynn, R., Barr, A., Fernandez-Valverde, F. (2017) Use of geographical information system-based hydrological modelling for development of a raised bog conservation and restoration programme. *Ecological Engineering*, 106, 242–252.

Mäkilä, M., Moisanen, M. (2007) Holocene lateral expansion and carbon accumulation of Luovuoma, a northern fen in Finnish Lapland. *Boreas*, 36, 198–210.

Minayeva, T.Yu., Bragg, O.M., Sirin, A.A. (2017) Towards ecosystem-based restoration of peatland biodiversity. *Mires and Peat*, 19, 01, 36 pp.

Nagano, T., Osawa, K., Ishida, T., Sakai, K., Vijarnsorn, P., Jongskul, A., Phetsuk, S., Waijaroen, S., Yamanoshita, T., Norisada, M., Kojima, K. (2013) Subsidence and soil CO_2 efflux in tropical peatland in southern Thailand under various water table and management conditions. *Mires and Peat*, 11, 06, 20 pp.

Notebaert, B., Verstraeten, G., Govers, G., Poesen, J. (2010) Quantification of alluvial sediment storage in contrasting environments: Methodology and error estimation. *Catena*, 82(3), 169–182.

Phys, P., Renaud, G., Rep, S.S., Hanebuth, T., Stattegger, K., Grootes, P.M. (2000) Rapid flooding of the Sunda Shelf: a late-glacial sea-level record. *Science*, 288, 1033–1036.

Post, V.E.A, Groen, J., Kooi, H., Person, M., Ge, S., Edmunds, M. (2013) Offshore fresh groundwater reserves as a global phenomenon. *Nature*, 504, 71–78.

Radjagukguk, B., Hastuti, S., Kurnain, A., Sajarwan, A., Kurniawan, R.E.K. (2000) *Panduan Analisis Laboratorium untuk Pambut* (*Laboratory Analysis Guide for Peat*). Uni Eropa - Universitas Gadjah Mada, Yogyakarta, 52 pp. (in Indonesian).

Rieley, J.O., Banks, C.J., Page, S.E. (2011) Global and regional importance of the tropical peatland carbon pool. *Global Change Biology*, 17(2), 798–818.

Sabiham, S., Basuki, S. (1989) Studies on peat in the coastal plains of Sumatra and Borneo part II: the clay mineralogical composition of sediments in coastal plains of Jambi and South Kalimantan. *Southeast Asian Studies*, 27(1), 35–54.

Sangireddy, H., Carothers, R.A., Stark, C.P., Passalacqua, P. (2016) Controls of climate, topography, vegetation, and lithology on drainage density extracted from high resolution topography data. *Journal of Hydrology*, 537, 271–282.

Simpson, J.E., Wooster, M.J., Smith, T.E.L., Trivedi, M., Vernimmen, R.R.E., Dedi, R., Shakti, M., Dinata, Y. (2016) Tropical peatland burn depth and combustion heterogeneity assessed using UAV photogrammetry and airborne LiDAR. *Remote Sensing*, 8, 1000, 1–21.

Smith, K. (ed.) (2015) *The Sago Palm: The Food and Environmental Challenges of the 21st Century*. Edited by The Society of Sago Palm Studies. Kyoto University Press, Kyoto and Trans Pacific Press, Melbourne, 450 pp.

Sorensen, K.W. (1993) Indonesian peat swamp forests and their role as a carbon sink. *Chemosphere*, 27(6), 1065–1082.

Strack, M., Waddington, J.M., Bourbonniere, R.A., Buckton, E.L., Shaw, K., Whittington, P., Price, J.S. (2008) Effect of water table drawdown on peatland dissolved organic carbon export and dynamics. *Hydrological Processes*, 22, 3700–3713.

Supardi, Subekty, A.D., Neuzil, S.G. (1993) General geology and peat resources of the Siakkanan and

15

Bengkalis Island peat deposits, Sumatra, Indonesia. In: Cobb, J.C., Cecil, C.B. (eds.) *Modern and Ancient Coal-Forming Environments*, Special Paper 286, The Geological Society of America, Boulder CO, 45–62.

Tata, H.L. (2019) Mixed farming systems on peatlands in Jambi and Central Kalimantan provinces, Indonesia: should they be described as paludiculture? *Mires and Peat*, 25, 08, 17 pp.

Trimble, S.W. (2008) The use of historical data and artifacts in geomorphology. *Progress in Physical Geography*, 32(1), 3–29.

Utami, S.H.U., Maas, A., Haerani, A., Anwar, K. (2014) Uji cepat monitoring kualitas tanah dan air di lingkungan rawa (Quick methods to determine soil and water quality in swamp environments). In: Maas, A. (ed.) *Pengelolaan Lahan Rawa untuk Pertanian* (*Management of Swampland for Agriculture*), Faculty of Agriculture, Universitas Gadjah Mada, Yogyakarta, 43–54 (in Indonesian).

Vernimmen, R., Hooijer, A., Yuherdha, A.T., Visser, M., Pronk, M., Eilander, D., Akmalia, R., Fitranatanegara, N., Mulyadi, D., Andreas, H., Ouellette, J., Hadley, W. (2019) Creating a lowland and peatland landscape digital terrain model (DTM) from interpolated partial coverage LiDAR data for Central Kalimantan and East Sumatra, Indonesia. *Remote Sensing*, 11, 1152, 16 pp.

Voris, H.K. (2017) Maps of Pleistocene sea levels in Southeast Asia: shorelines, river systems and time durations. *Journal of Biogeography*, 27(5), 1153–1167.

Walter, J., Lück, E., Bauriegel, A., Facklam, M., Zeitz, J. (2018) Seasonal dynamics of soil salinity in peatlands: A geophysical approach. *Geoderma*, 310, 1–11.

Whitten, T., Damanik, S.J., Anwar, J., Hisyam, N. (2000) *The Ecology of Sumatra*. The Ecology of Indonesia Volume 1, Oxford University Press, 72–73.

Wu, R.A.J., Bustin, R.M. (2004) Late Pleistocene and Holocene development of the interior peat-accumulating basin of tropical Tasek Bera, Peninsular Malaysia. *Palaeogeography, Palaeoclimatology, Palaeoecology*, 211, 241–270.

Young, D.M., Parry, L.E., Lee, D., Ray, S. (2018) Spatial models with covariates improve estimates of peat depth in blanket peatlands. *Plos One*, 13(9), 1–19.

Author for correspondence:
Dr Sri Nuryani Hidayah Utami, Department of Soil Science, Faculty of Agriculture, Universitas Gadjah Mada, Bulaksumur, Yogyakarta 55281, Indonesia. Tel. +62-815-6807-552; Email: nuryani@ugm.ac.id

16

Appendix

Table A1. Locations of survey points and data collected for characterisation of peat thickness and of the mineral substratum. Shaded cells indicate survey points without peat that were eliminated from the statistical analysis.

No.	Location of survey point			Surface altitude (m a.s.l)	Peat thickness (m)	Peat maturity	Bulk density (g cm^{-3})	Water Content (% of wet weight)	Ash content (%)	Substratum (texture, pH)
	Point ID	° North	° East							
1	CS1_1	0.9972	102.7814	4.60	0.00	-	-	-	-	-
2	CS1_2	0.9933	102.7793	4.50	0.00	-	-	-	-	-
3	CS1_3	0.9893	102.7771	4.00	0.00	-	-	-	-	-
4	CS1_4	0.9814	102.7727	4.00	0.00	-	-	-	-	-
5	CS1_5	0.9775	102.7704	3.70	0.00	-	-	-	-	-
6	CS1_6	0.9736	102.7684	4.00	0.00	-	-	-	-	-
7	CS1_7	0.9696	102.7662	4.70	1.80	sapric; hemic	-	-	-	-
8	CS1_8	0.9657	102.7640	5.00	1.60	sapric; hemic	-	-	-	-
9	CS1_9	0.9617	102.7619	5.00	1.85	sapric; hemic	-	-	-	-
10	CS1_10	0.9581	102.7598	5.50	2.18	hemic; fibric	-	-	-	-
11	CS1_11	0.9538	102.7575	6.50	4.00	hemic; fibric	-	-	-	-
12	CS1_12	0.9459	102.7531	7.00	4.20	hemic; fibric	-	-	-	-
13	CS1_13	0.9420	102.7509	6.80	4.70	I. sapric II. hemic III. fibric IV. fibric	0.14 0.18 0.19 0.14	74.22 85.33 89.85 89.20	0.95 2.31 2.80 4.67	clay, 5.0
14	CS1_14	0.9380	102.7488	7.00	4.80	hemic; fibric	-	-	-	-
15	CS1_15	0.9341	102.7466	6.80	4.60	hemic; fibric	-	-	-	-
16	CS1_16	0.9303	102.7436	6.00	1.80	sapric; hemic	-	-	-	-
17	CS1_17	0.9262	102.7422	5.30	0.85	I. hemic II. fibric	0.17 0.15	86.78 88.25	1.56 1.98	clay, 2.0
18	CS1_18	0.9223	102.7401	3.50	0.20	sapric	-	-	-	-
19	CS1_19	0.9208	102.7379	0.00	0.00	-	-	-	-	-

No.	Location of survey point			Surface altitude (m a.s.l)	Peat thickness (m)	Peat maturity	Bulk density (g cm^{-3})	Water Content (% of wet weight)	Ash content (%)	Substratum (texture, pH)
	Point ID	° North	° East							
20	CS1_20	0.9099	102.7364	0.00	0.00	-	-	-	-	-
21	CS1_21	0.9065	102.7313	4.40	0.00	-	-	-	-	-
22	CS1_22	0.9026	102.7291	4.50	0.00	-	-	-	-	-
23	CS1_23	0.8989	102.7271	5.50	2.73	sapric; hemic	-	-	-	-
24	CS1_24	0.8947	102.7248	6.00	2.53	sapric; hemic	-	-	-	-
25	CS1_25	0.8907	102.7227	8.00	5.42	hemic; fibric	-	-	-	-
26	CS1_26	0.8871	102.7205	9.50	7.74	hemic; fibric	-	-	-	-
27	CS1_27	0.8828	102.7183	10.00	7.38	hemic; fibric	-	-	-	-
28	CS1_28	0.8788	102.7161	9.50	9.10	sapric; hemic	-	-	-	-
29	CS1_29	0.8750	102.7139	9.50	8.32	sapric; hemic	-	-	-	-
30	CS1_30	0.8710	102.7117	9.50	8.21	sapric; hemic	-	-	-	-
31	CS1_31	0.8671	102.7096	9.50	9.34	sapric; hemic	-	-	-	-
32	CS1_32	0.8631	102.7073	10.00	10.28	hemic; fibric	-	-	-	-
33	CS1_33	0.8591	102.7052	10.00	9.50	sapric; hemic	-	-	-	-
34	CS1_34	0.8552	102.7031	10.00	10.11	sapric; hemic	-	-	-	-
35	CS1_35	0.8512	102.7009	10.00	10.40	I. sapric II. hemic	0.12 0.13	90.0 90.46	1.62 1.53	silty clay, 2.5
36	CS1_36	0.8473	102.6987	10.00	10.33	sapric; hemic	-	-	-	-
37	CS1_37	0.8437	102.6962	9.50	10.01	fibric; hemic	-	-	-	-
38	CS1_38	0.8394	102.6943	9.50	7.40	hemic; fibric	-	-	-	-
39	CS1_39	0.8354	102.6921	9.50	4.50	hemic; fibric	-	-	-	-
40	CS1_40	0.8315	102.6900	9.50	7.70	hemic; fibric	-	-	-	-
41	CS1_41	0.8276	102.6878	9.50	8.12	hemic; fibric	-	-	-	-
42	CS1_42	0.8236	102.6856	9.50	6.54	hemic; fibric	-	-	-	-
43	CS1_43	0.8197	102.6834	9.50	7.50	hemic; fibric	-	-	-	-
44	CS1_44	0.8157	102.6812	9.40	6.80	hemic; fibric	-	-	-	-

18

No.	Location of survey point			Surface altitude (m a.s.l)	Peat thickness (m)	Peat maturity	Bulk density (g cm⁻³)	Water Content (% of wet weight)	Ash content (%)	Substratum (texture, pH)
	Point ID	° North	° East							
45	CS1_45	0.8118	102.6791	9.20	5.60	hemic; fibric	-	-	-	-
46	CS1_46	0.8078	102.6769	8.60	4.99	hemic; fibric	-	-	-	-
47	CS1_47	0.8039	102.6747	7.90	4.61	hemic; fibric	-	-	-	-
48	CS1_48	0.7999	102.6725	6.60	2.70	I. hemic II. fibric III. fibric	0.26 0.19 0.17	74.78 85.16 87.16	- - 2.57	clay, 3.5
49	CS1_49	0.7960	102.6704	5.70	1.47	hemic; fibric	-	-	-	-
50	CS1_50	0.7920	102.6682	4.90	1.12	hemic; fibric	-	-	-	-
51	CS2_1	0.9313	102.8990	5.50	2.25	sapric	-	-	-	-
52	CS2_2	0.9272	102.8967	5.70	2.25	sapric	-	-	-	-
53	CS2_3	0.9231	102.8946	6.00	3.25	fibric	-	-	-	-
54	CS2_4	0.9198	102.8922	6.00	4.72	sapric	-	-	-	-
55	CS2_5	0.9154	102.8904	5.60	4.00	I. sapric II. hemic	0.25 0.16	64.72 88.56		sandy clay, 2.5
56	CS2_6	0.9117	102.8881	6.00	3.57	sapric; hemic	-	-	-	-
57	CS2_7	0.9078	102.8860	7.00	3.45	sapric; hemic	-	-	-	-
58	CS2_8	0.9038	102.8838	7.50	3.14	sapric; hemic	-	-	-	-
59	CS2_9	0.8999	102.8816	8.00	8.32	sapric; hemic	-	-	-	-
60	CS2_10	0.8960	102.8794	8.50	7.95	hemic; fibric	-	-	-	-
61	CS2_11	0.8920	102.8772	8.80	8.70	I. sapric II. hemic III. fibric	0.16 0.16 0.22	85.34 86.81 83.39	3.13 3.57 1.50	silt, 3.8
62	CS2_12	0.8881	102.8751	9.20	8.20	sapric; hemic	-	-	-	-
63	CS2_13	0.8841	102.8729	9.50	8.53	sapric; hemic	-	-	-	-
64	CS2_14	0.8802	102.8707	10.00	6.40	hemic; fibric	-	-	-	-
65	CS2_15	0.8762	102.8685	10.30	7.65	sapric; hemic	-	-	-	-

No.	Location of survey point			Surface altitude (m a.s.l)	Peat thickness (m)	Peat maturity	Bulk density (g cm⁻³)	Water Content (% of wet weight)	Ash content (%)	Substratum (texture, pH)
	Point ID	° North	° East							
66	CS2_16	0.8723	102.8664	10.30	7.91	sapric; hemic	-	-	-	-
67	CS2_17	0.8683	102.8642	10.50	8.14	hemic; fibric	-	-	-	-
68	CS2_18	0.8644	102.8620	10.50	7.91	hemic; fibric	-	-	-	-
69	CS2_19	0.8604	102.8598	10.50	8.11	I. hemic II. fibric	0.16 0.11	86.59 91.4	1.11 1.66	silty clay, 2.0
70	CS2_20	0.8564	102.8576	10.50	7.50	sapric; hemic	-	-	-	-
71	CS2_21	0.8526	102.8555	10.30	8.30	sapric; hemic	-	-	-	-
72	CS2_22	0.8486	102.8533	10.00	7.20	sapric; hemic	-	-	-	-
73	CS2_23	0.8443	102.8498	10.00	8.00	hemic; fibric	-	-	-	-
74	CS2_24	0.8407	102.8498	10.00	8.00	sapric; hemic	-	-	-	-
75	CS2_25	0.8372	102.8465	9.50	7.70	hemic; fibric	-	-	-	-
76	CS2_26	0.8330	102.8445	9.50	7.00	sapric; hemic	-	-	-	-
77	CS2_27	0.8289	102.8437	9.50	7.20	sapric; hemic	-	-	-	-
78	CS2_28	0.8241	102.8402	9.30	6.00	hemic; fibric	-	-	-	-
79	CS2_29	0.8192	102.8386	9.00	6.30	hemic; fibric	-	-	-	-
80	CS2_30	0.8170	102.8359	8.50	5.17	hemic; fibric	-	-	-	-
81	CS2_31	0.8131	102.8337	8.00	5.13	hemic; fibric	-	-	-	-
82	CS2_32	0.8091	102.8315	7.50	3.43	sapric; hemic	-	-	-	-
83	CS2_33	0.8051	102.8293	7.00	3.26	sapric; hemic	-	-	-	-
84	CS2_34	0.7998	102.8268	6.00	0.00	-	-	-	-	-
85	CS2_35	0.7973	102.8250	5.50	0.00	-	-	-	-	-
86	CS2_36	0.7933	102.8228	5.00	0.00	-	-	-	-	-
87	LS_1	0.9114	102.4270	2.40	0.00	-	-	-	-	-
88	LS_2	0.9114	102.4270	2.50	0.00	-	-	-	-	-
89	LS_3	0.9054	102.4536	8.00	6.15	-	-	-	-	-

No.	Location of survey point			Surface altitude (m a.s.l)	Peat thickness (m)	Peat maturity	Bulk density (g cm⁻³)	Water Content (% of wet weight)	Ash content (%)	Substratum (texture, pH)
	Point ID	° North	° East							
90	LS_4	0.9014	102.4821	8.50	9.33	I. sapric II. hemic III. fibric	0.19 0.19 0.16	80.24 84.77 86.87	0.15 1.04 1.19	clay, 4.7
91	LS_5	0.8960	102.5101	10.40	8.64	sapric; hemic	-	-	-	-
92	LS_6	0.8908	102.5379	11.30	12.10	sapric; hemic	-	-	-	-
93	LS_7	0.8855	102.5657	11.50	9.72	I. hemic II. fibric	0.11 0.17	87.56 85.82	2.1 2.89	silt, 2.5
94	LS_8	0.8803	102.5937	9.65	7.32	hemic; fibric	-	-	-	-
95	LS_9	0.8723	102.6194	0.00	0.00	-	-	-	-	-
96	LS_10	0.8698	102.6491	9.20	7.00	hemic; fibric	-	-	-	-
97	LS_11	0.8643	102.6773	10.00	5.59	sapric; hemic	-	-	-	-
98	LS_12	0.8591	102.7052	10.00	9.50	hemic; fibric	-	-	-	-
99	LS_13	0.8538	102.7331	10.00	10.25	I. hemic II. fibric	0.17 0.09	87.41 93.4	2.02 2.59	silty clay, 2.5
100	LS_14	0.8486	102.7609	9.50	7.36	sapric; hemic	-	-	-	-
101	LS_15	0.8424	102.7888	9.00	6.10	sapric; hemic	-	-	-	-
102	LS_16	0.8375	102.8166	9.50	5.10	sapric; hemic	-	-	-	-
103	LS_17	0.8330	102.8445	9.50	7.00	hemic; fibric	-	-	-	-
104	LS_18	0.8275	102.8720	9.80	5.35	hemic; fibric	-	-	-	-
105	LS_19	0.8223	102.9004	10.50	6.20	sapric; hemic	-	-	-	-
106	LS_20	0.8165	102.9280	9.30	6.50	I. hemic II. fibric	0.16 0.11	86.59 91.4	2.08	silty clay, 2.0
107	LS_21	0.8117	102.9560	9.10	6.09	sapric; hemic	-	-	-	-
108	LS_22	0.8073	102.9840	10.00	5.90	hemic; fibric	-	-	-	-
109	LS_23	0.8017	103.0121	9.50	5.80	I. hemic II. fibric	0.26 0.13	78.36 90.74		clay, 2.5
110	LS_24	0.7963	103.0394	7.00	0.65	sapric	-	-	-	-